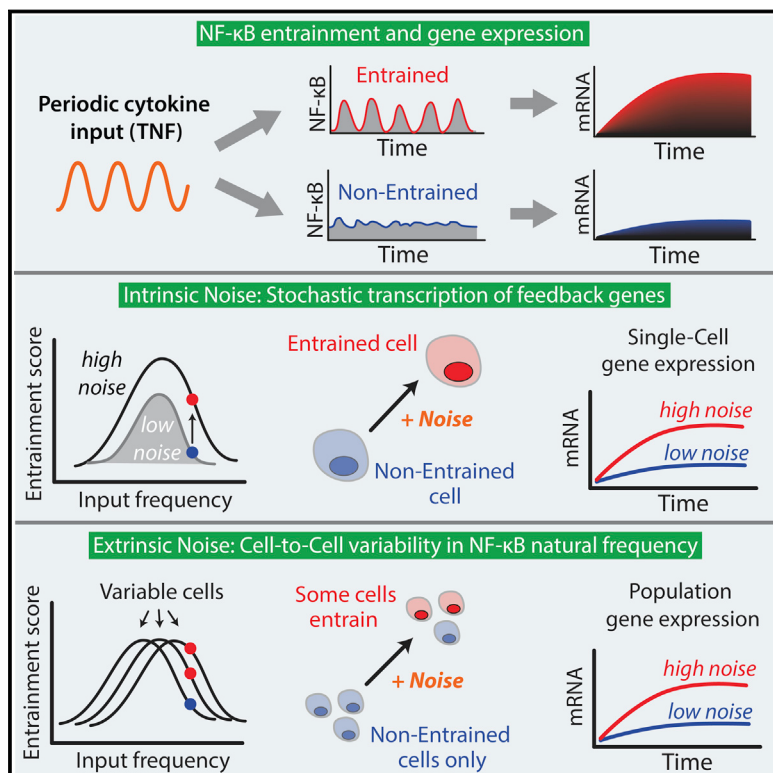


# Noise Facilitates Transcriptional Control under Dynamic Inputs

## Graphical Abstract



## Authors

Ryan A. Kellogg, Savaş Tay

## Correspondence

savas.tay@bsse.ethz.ch

## In Brief

Intrinsic biochemical noise in individual cells, traditionally considered as harmful to signal transduction, improves NF-κB oscillation and entrainment, whereas cell-to-cell variability in NF-κB natural frequency creates population robustness. Together, the two types of transcriptional noise enable signal entrainment over a wider range of dynamic inputs.

## Highlights

- Periodic TNF stimulation entrains and amplifies NF-κB oscillations
- Amplified NF-κB oscillation increases transcriptional efficiency
- Intrinsic biochemical noise improves oscillation and entrainment of single cells
- Extrinsic noise allows population to entrain robustly under a wider range of inputs

# Noise Facilitates Transcriptional Control under Dynamic Inputs

Ryan A. Kellogg<sup>1</sup> and Savaş Tay<sup>1,\*</sup>

<sup>1</sup>Department of Biosystems Science and Engineering, ETH Zürich 4058, Switzerland

\*Correspondence: [savas.tay@bsse.ethz.ch](mailto:savas.tay@bsse.ethz.ch)

<http://dx.doi.org/10.1016/j.cell.2015.01.013>

## SUMMARY

**Cells must respond sensitively to time-varying inputs in complex signaling environments. To understand how signaling networks process dynamic inputs into gene expression outputs and the role of noise in cellular information processing, we studied the immune pathway NF-κB under periodic cytokine inputs using microfluidic single-cell measurements and stochastic modeling. We find that NF-κB dynamics in fibroblasts synchronize with oscillating TNF signal and become entrained, leading to significantly increased NF-κB oscillation amplitude and mRNA output compared to non-entrained response. Simulations show that intrinsic biochemical noise in individual cells improves NF-κB oscillation and entrainment, whereas cell-to-cell variability in NF-κB natural frequency creates population robustness, together enabling entrainment over a wider range of dynamic inputs. This wide range is confirmed by experiments where entrained cells were measured under all input periods. These results indicate that synergy between oscillation and noise allows cells to achieve efficient gene expression in dynamically changing signaling environments.**

## INTRODUCTION

Understanding how cells efficiently process information in rapidly changing and noisy environments is a fundamental problem in biology. Cells experience environments that fluctuate over time during physiological conditions such as inflammation, where oscillating input signals can occur due to pulsatile secretion of signaling molecules from immune cells (Goldbeter et al., 1990; Han et al., 2012), propagating signaling waves (Falcke, 2003; Schütze et al., 2011; Yde et al., 2011), or by coupling between upstream pathways (Gérard and Goldbeter, 2012; Goldbeter and Pourquié, 2008; Yang et al., 2010; Yoshiura et al., 2007). How cells process such dynamic inputs into functional gene expression outputs is not well understood. Further, signaling systems are subject to biochemical noise originating from stochastic molecular interactions, leading to system noise and cell-to-cell variability in response to input signals. While it is a common belief that noise is harmful to information processing (Cheong et al., 2011), cell signaling pathways perform with

remarkable robustness despite ever-present system noise and variability (Little et al., 1999). It is not clear how cell-signaling pathways overcome system noise and whether there are functional roles for noise in cellular information processing.

Signaling systems often employ oscillatory network architecture to process environmental inputs (Levine et al., 2013). For example, specific transcriptional responses can be achieved by encoding the dose or identity of a constant input signal by modulating oscillatory response dynamics (Kupzig et al., 2005). Theoretically, oscillation can be advantageous also in the processing of fluctuating and noisy input signals. For example, dynamic inputs that contain noise can be transmitted efficiently in an oscillating system through a phenomenon called stochastic resonance (Douglass et al., 1993), previously observed in neuronal circuits (McDonnell and Ward, 2011). Nevertheless, such a beneficial role for biochemical system noise in the processing of fluctuating environmental signals has not been shown.

To study how oscillation and system noise may interact in processing of dynamic input signals, we consider the NF-κB system, a gene regulatory network central to immune functions and many diseases, including autoimmunity and cancer (Hayden and Ghosh, 2008). NF-κB pathway activation by TNF cytokine leads to oscillations in p65:p50 heterodimer localization between the cytoplasm and nucleus (Hayden and Ghosh, 2008; Hoffmann et al., 2002; Nelson et al., 2004), mediated by NF-κB-dependent induction of negative feedback genes of the IκB family (Figure 1A). Pathway activation through IKK under TNF occurs in a digital, switch-like fashion (Tay et al., 2010).

NF-κB oscillations are subject to intrinsic and extrinsic noise, leading to variable timing between cells that obscures single-cell behavior in population analyses (Swain et al., 2002; Tay et al., 2010). Sources of extrinsic noise include different signaling histories and uneven cell division leading to variation in protein abundance (Huh and Paulsson, 2011). Variation in TNF receptor or NF-κB molecules create different response characteristics between cells (Tay et al., 2010). Significant contributions to intrinsic (biochemical) noise in NF-κB include burst-like transcription of IκB and A20 negative feedback genes, and receptor-ligand interaction at low ligand concentration (Elovitz et al., 2002; Tay et al., 2010). Another negative feedback gene IκBε is induced with a 45 min delay compared to IκBα, which is optimally timed for increasing cell-to-cell oscillation variability, suggesting that transcriptional noise might provide a functional advantage (Ashall et al., 2009; Paszek et al., 2010).

The function of NF-κB oscillation is not fully understood. Other pathways like p53 and Notch convert between oscillatory and

non-oscillatory response to achieve specific cell fate responses (Dolmetsch et al., 1998; Kageyama et al., 2008; Purvis et al., 2012; Purvis and Lahav, 2013). The frequency of oscillation in ERK, Crz1, and NFAT4 is altered depending on input signal concentration, achieving expression control across diverse promoters through frequency modulation (Albeck et al., 2013; Berridge et al., 2003; Cai et al., 2008; Dolmetsch et al., 1998; Eldar and Elowitz, 2010; Shankaran et al., 2009; Yissachar et al., 2013). However, NF- $\kappa$ B oscillation frequency (90 to 100 min peak-to-peak interval) is unchanged across a wide range of input concentrations (Longo et al., 2013; Tay et al., 2010; Turner et al., 2010), and it is uncertain how NF- $\kappa$ B oscillation changes and directs gene expression in response to a fluctuating input.

Oscillatory systems can experience resonance, where a periodic stimulus leads to amplified output (Abraham et al., 2010; Pikovsky et al., 2003). Periodic input may also entrain or synchronize a population of oscillators so that all oscillators adopt the same frequency and phase. Entrainment leading to resonant amplification of NF- $\kappa$ B oscillations may occur for input signals that fluctuate at a rate similar to the NF- $\kappa$ B natural frequency, increasing the sensitivity of the NF- $\kappa$ B system especially to small signals. Theoretical studies predict that periodic input to NF- $\kappa$ B may generate entrainment, quasiperiodic oscillations, or even chaos (Jensen and Krishna, 2012; Wang et al., 2011). Entrainment, with prominent examples from circadian rhythms and brain waves, allows oscillatory signaling and transcriptional pathways to synchronize and work in harmony (Reppert and Weaver, 2002; Varela et al., 2001). It is conceivable that entrainment could reduce cell-to-cell NF- $\kappa$ B oscillation variability, leading to homogenous transcriptional responses at the population level. Nevertheless, experimental studies are lacking on whether NF- $\kappa$ B can experience resonance and entrainment, and whether there is impact on gene expression output and variability (Longo et al., 2013; Tay et al., 2010; Turner et al., 2010).

Although noise is detrimental to signal transmission in linear systems, it can facilitate information transfer in a non-linear system by decreasing the amplitude of a periodic input needed to achieve coupling (Collins et al., 1996; Lindner et al., 2004; Mori and Kai, 2002; Zhou et al., 2002). For example, input noise can facilitate sensory neuron processing (McDonnell and Ward, 2011) and intrinsic noise may cause oscillations to become more robust to perturbation (Paszek et al., 2010; Perc and Marhl, 2003; Vilar et al., 2002). Extrinsic noise (i.e., variation in signaling parameters between cells) may also impact entrainment due to increased population diversity, similar to bacterial bet hedging when external conditions change (Mondragón-Palomino et al., 2011; Suel et al., 2006; Wakamoto et al., 2013). However, it is not known how noise could affect entrainment of a complex and physiological mammalian system such as NF- $\kappa$ B.

To probe how oscillation and noise together determine NF- $\kappa$ B-dependent transcription in dynamic settings, we used a microfluidics-based experimental pipeline that enabled automated cell stimulation, live imaging, and gene expression measurements (Gómez-Sjöberg et al., 2007; Junkin and Tay, 2014; Kellogg et al., 2014; Tay et al., 2010). We delivered various TNF cytokine inputs to p65<sup>-/-</sup> mouse 3T3 fibroblast cells expressing p65/DsRed fusion protein at near wild-type levels (Lee et al.,

2009; Tay et al., 2010) (Figures 1B and 2A and 3A). The microfluidic chip utilizes computer controlled PDMS membrane valves, allowing constant perfusion or periodic pulsing of signaling factors. Ninety-six independent cell culture experiments each with complex fluidic conditions can be maintained in parallel. Cell images acquired at 5 min intervals were automatically analyzed, extracting thousands of single-cell trajectories of NF- $\kappa$ B nuclear intensity over time (Kellogg et al., 2014). Following periodic TNF stimulation, cells were retrieved for gene expression analysis in a high-throughput microfluidic qPCR system to understand the influence of entrainment on target gene expression (Kellogg et al., 2014). Furthermore, we performed stochastic simulations using an established model of NF- $\kappa$ B (Tay et al., 2010) and varied both intrinsic and extrinsic noise to interpret our experimental findings and understand the role of noise and oscillations for NF- $\kappa$ B dynamic signal processing.

## RESULTS

### Constant TNF Stimulation Generates Sustained, Noisy NF- $\kappa$ B Oscillations

Previous studies of NF- $\kappa$ B dynamics were subject to TNF ligand loss due to degradation and cellular internalization, leading to damped oscillations (Tay et al., 2010). Here, constant TNF concentration was achieved by perfusion of fresh TNF-containing media using an on-chip peristaltic pump (Figure 1B). Under constant TNF concentration, we observed NF- $\kappa$ B oscillations sustaining longer than 24 hr with mean period approximately 90 min (Figures 1C and 1D and Movie S1). Cells exhibited different natural frequencies (between-cell variability) and cycle-to-cycle timing fluctuation (within-cell variability) (Figure 1F). NF- $\kappa$ B oscillation is robust to changes in dose, and lowered dose, which generates high receptor-ligand noise, modestly lengthened the average period and increased period variability (CV: coefficient of variation, in Figure 1E). These findings show that NF- $\kappa$ B oscillation sustains under constant TNF input, pointing to a conserved function for oscillations.

To understand how noise underlies oscillation variability, we performed simulations of NF- $\kappa$ B dynamics under constant TNF concentration. We used a stochastic single-cell model, which faithfully reproduces the NF- $\kappa$ B dynamics in single 3T3 fibroblast cells used in this study (Tay et al., 2010). The simulations showed sustained oscillation and period characteristics similar to our experiments (Figure 1G) (Lipniacki et al., 2004; Lipniacki et al., 2007; Tay et al., 2010). Varying intrinsic noise in the model associated with changes in cycle-to-cycle variability, while changing extrinsic noise affected variability in average (natural) oscillation period between cells (Figures 1G and 1H). Magnitudes of variability for simulations matched that of experimental measurements, supporting an appropriate balance between intrinsic and extrinsic noise in the model (Figure 1I).

### Single-Cell NF- $\kappa$ B Dynamics becomes Entrained under an Oscillating Cytokine Signal

During inflammation cells operate under dynamic TNF signals, which may interfere with NF- $\kappa$ B oscillations needed for processing of input dose information and differential gene expression (Tay et al., 2010). Depending on frequency and amplitude,

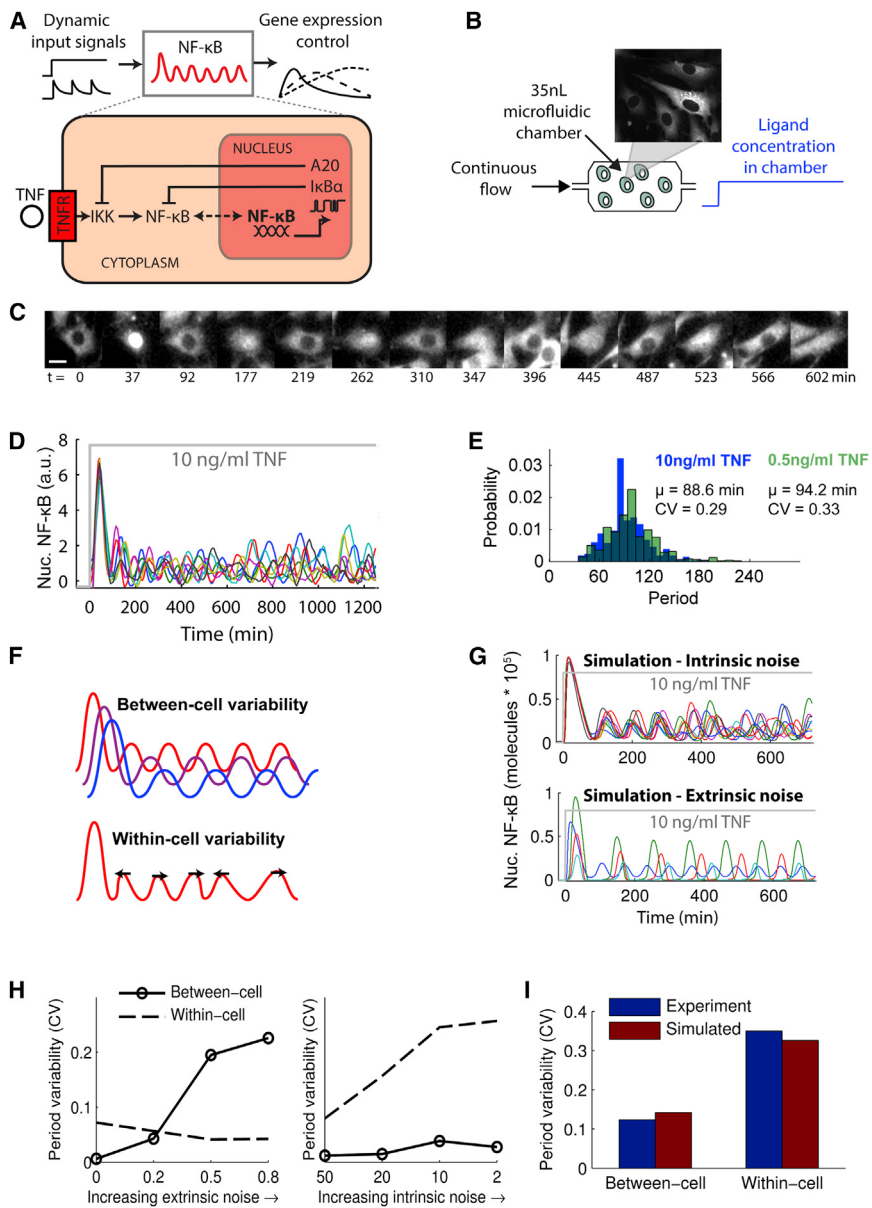


**Figure 1. Noise Origins of Sustained NF-κB Oscillation and Heterogeneity**

(A) NF-κB transcription factor oscillates between cytoplasm and nucleus in response to inflammatory signals. NF-κB dynamics relay external signals to gene expression outputs.

(B) We deliver continuous or periodic inputs to cells using microfluidic cell culture. In continuous mode, TNF is flowed over cells to maintain constant concentration.

(C) We record single-cell NF-κB translocation using live-cell microscopy. Images show nucleus-cytoplasm oscillations in NF-κB (p65-dsRed) under continuous TNF perfusion. Scale bar, 10 μm.

(D) Under constant 10 ng/ml TNF concentration, NF-κB shows long sustaining, asynchronous oscillations.

(E) NF-κB oscillates with mean period ~90 min under constant high and low dose input ( $n = 40$  cells).

(F) Pictorial depiction of within- and between-cell oscillation variability. While cells may have different mean periods (between-cell variability), each cell also exhibits fluctuation in its own oscillation (within-cell variability).

(G) Simulated single cell trajectories show that extrinsic noise increases between-cell variability, and intrinsic noise increases within-cell variability.

(H) In simulations increasing extrinsic noise increases between-cell variability, while increasing intrinsic noise increases within-cell variability.

(I) Experimentally, we observe ~12% period fluctuation between different cells and 34% within the same cells under 10 ng/ml TNF. Variability in simulated traces agrees with experimentally measured values.

periodic input to an oscillator like NF-κB can either entrain or disrupt the oscillation. Entrainment describes when the oscillator becomes phase-locked and synchronized with the driving stimuli (Pikovsky et al., 2003), with prominent examples in biology from circadian rhythms (Leloup and Goldbeter, 2003; Reppert and Weaver, 2002) and brain waves, to synthetic bacterial oscillators (Mondragón-Palomino et al., 2011). On the other hand, when entrainment cannot occur due a significant frequency mismatch between the oscillator and input signal, the result is a disrupted oscillation that is quasiperiodic or even chaotic (Jensen and Krishna, 2012; Pikovsky et al., 2003). How NF-κB responds to sustained periodic inputs that could entrain NF-κB oscillations has not been experimentally investigated so far.

To test the entrainment capacity of NF-κB and how oscillation contributes to gene expression control under fluctuating cyto-

kin signals, we applied TNF inputs to fibroblasts using two stimulation periods (Figure 2A): in the first case, TNF stimulus is applied every 120 min, which indeed efficiently entrained NF-κB after a transient (Figure 2B). In the second case, TNF stimulus was provided every 60 min, which was sufficiently mismatched from the ~90 min NF-κB natural

period to induce a disrupted, non-entrained NF-κB response in most cells (Figure 2C). Movies S2, S3, and S4 show single-cells under these inputs as well as under 90 min input, and Figure S1 shows the difference between entrained cells and cells oscillating under constant TNF signal. Images selected at three time points show that for 60 min input NF-κB oscillations remain asynchronous in the population, and for 120 min input NF-κB oscillates synchronously across cells (Figures 2D and 2E, also see and Movies S2, S3, and S4). Population phase variability, a measure of synchrony, remains high during the time course with 60 min stimulation, but it quickly reduces during 120 min stimulation as the population entrains (Figures 2F and S1B). Simulations with our comprehensive NF-κB model also reproduced non-entrained and entrained responses under similar inputs (Figure 2G).

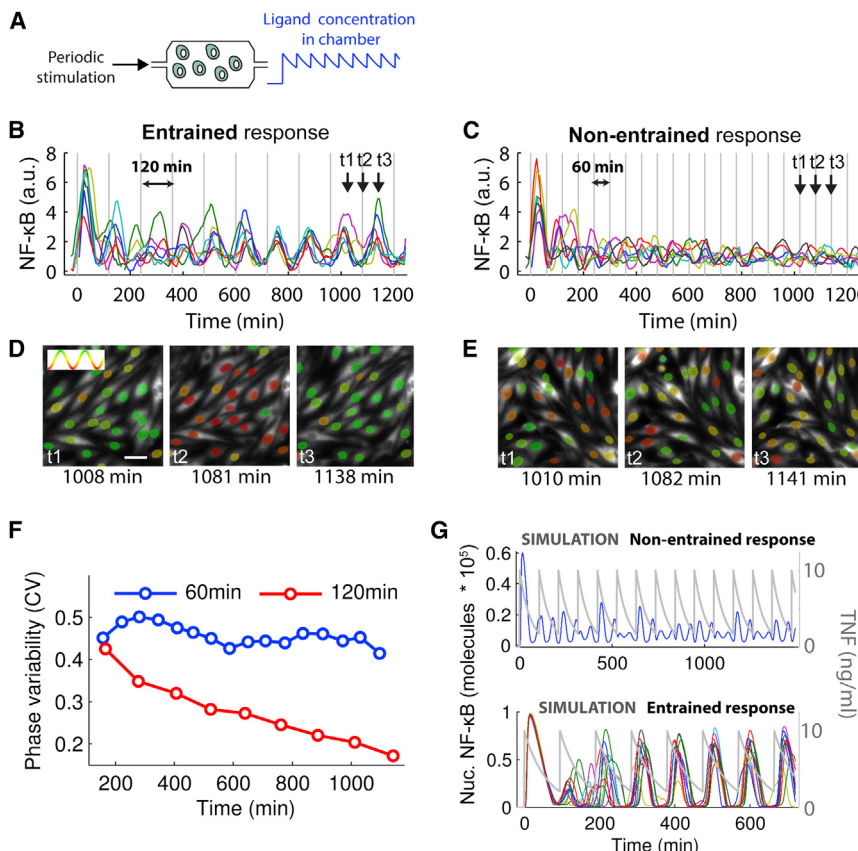


**Figure 2. Periodic TNF Stimulation Can Entrain or Disrupt NF-κB Oscillations**

(A) We deliver periodic inputs to cells using a microfluidic cell culture chip. In periodic mode, TNF is replaced at specified intervals, and ligand decay (due to cell uptake and degradation) leads to a periodic sawtooth concentration profile.

(B) Single-cell traces for stimulation at 120 min input period, which entrains and synchronizes NF-κB oscillations.

(C) Single-cell NF-κB trajectories measured for stimulation at 60 min input, which disrupts NF-κB oscillations.

(D) Image time-series for 120 min periodic input for times t<sub>1</sub>–t<sub>3</sub> indicated by arrows in B. The entrained cell population oscillates synchronously. Inset: Nucleus color indicates nuclear NF-κB intensity from red (low) to green (high). Scale bar, 25 μm.

(E) Image time series for 60 min periodic input for times t<sub>1</sub>–t<sub>3</sub> indicated by arrows in (B). The cell population does not synchronize.

(F) Phase variability for 60 min stimulation remains constant over time. In contrast, during 120 min stimulation (red), phase variability decreases as the cell population synchronizes over time.

(G) Simulations reproduce non-entrained and entrained responses. See also Figure S1.

### Entrained NF-κB Oscillation Improves Gene Expression Efficiency and Reduces Cell-to-Cell Variability

NF-κB regulates hundreds of pro- and anti-inflammatory genes (Hao and Baltimore, 2013). To understand the influence of entrained versus disorderly NF-κB dynamics in gene expression, we measured time-dependent expression of target genes for 120 min and 60 min periodic TNF stimulation using microfluidic qPCR (Figures 3A and 3B, S2, and S3). Cells stimulated in independent chambers of the cell culture chip were harvested for expression analysis at 30 min time increments (Figure 3A) (See protocols in Kellogg et al., 2014). Under the entraining 120 min input, gene expression output is notably enhanced, especially in genes with later induction times (Figure 3C, red lines). In contrast, 60 min input that leads to non-entrained NF-κB response caused an impaired transcriptional response (Figure 3C, blue lines). Importantly, the difference in measured mRNA expression is not due to a difference in total TNF exposure, as there is greater TNF exposure for 60 min input (Figure 3D).

We analyzed single-cell NF-κB trajectories for entrained and non-entrained conditions to identify what might give rise to the observed gene expression difference. Since differences are most evident in the later part of the time course, we focused our analysis to time after 500 min. We measured NF-κB area under the curve (AUC) and determined the extent that each trace is oscillatory versus non-oscillatory by power spectral analysis. The AUC is a measure of total NF-κB protein localization into the nucleus, which did not change in a significant way to explain

the observed gene expression difference. Entrained compared to non-entrained cells showed only 9% increase in NF-κB area. However, we measured 83% increase in NF-κB oscillatory energy (Figure 3E). Non-entraining input at 60 min mostly resulted in non-oscillatory localization profiles, while entraining input at 120 min resulted in strong oscillations with large amplitude (Figure 3F).

To understand how increased oscillation magnitude under entraining input could lead to higher transcriptional output, we simulated traces for 60 and 120 min sawtooth input, similar to those used in experiments. Simulated NF-κB single cells exhibited similar changes in area and oscillatory energy for entrained versus non-entrained conditions (Figures 3G and S2). However, the existing transcriptional model, which assumed that NF-κB binding to DNA increases linearly with nuclear NF-κB concentration (Tay et al., 2010), did not reproduce increased gene expression for the entrained condition (Figure S2). Experiments indicate that NF-κB binds DNA cooperatively with Hill coefficient ~4 (Phelps et al., 2000) (Figure S2A). Introducing this non-linearity in our model created significantly increased transcriptional output for entrained versus non-entrained conditions, in agreement with our experiments (Figures 3G and S2C) (Wee et al., 2012). Increasing intrinsic noise led to stronger oscillations and further amplified the NF-κB-induced gene expression (Figure 3G). Thus, entraining input leads to strengthening of NF-κB oscillations, which are further amplified by noise to drive increased transcriptional output.

We asked whether entrainment could reduce cell-to-cell variability in transcriptional output in our simulations. Comparing the coefficient of variation of mRNA output over time indicates that

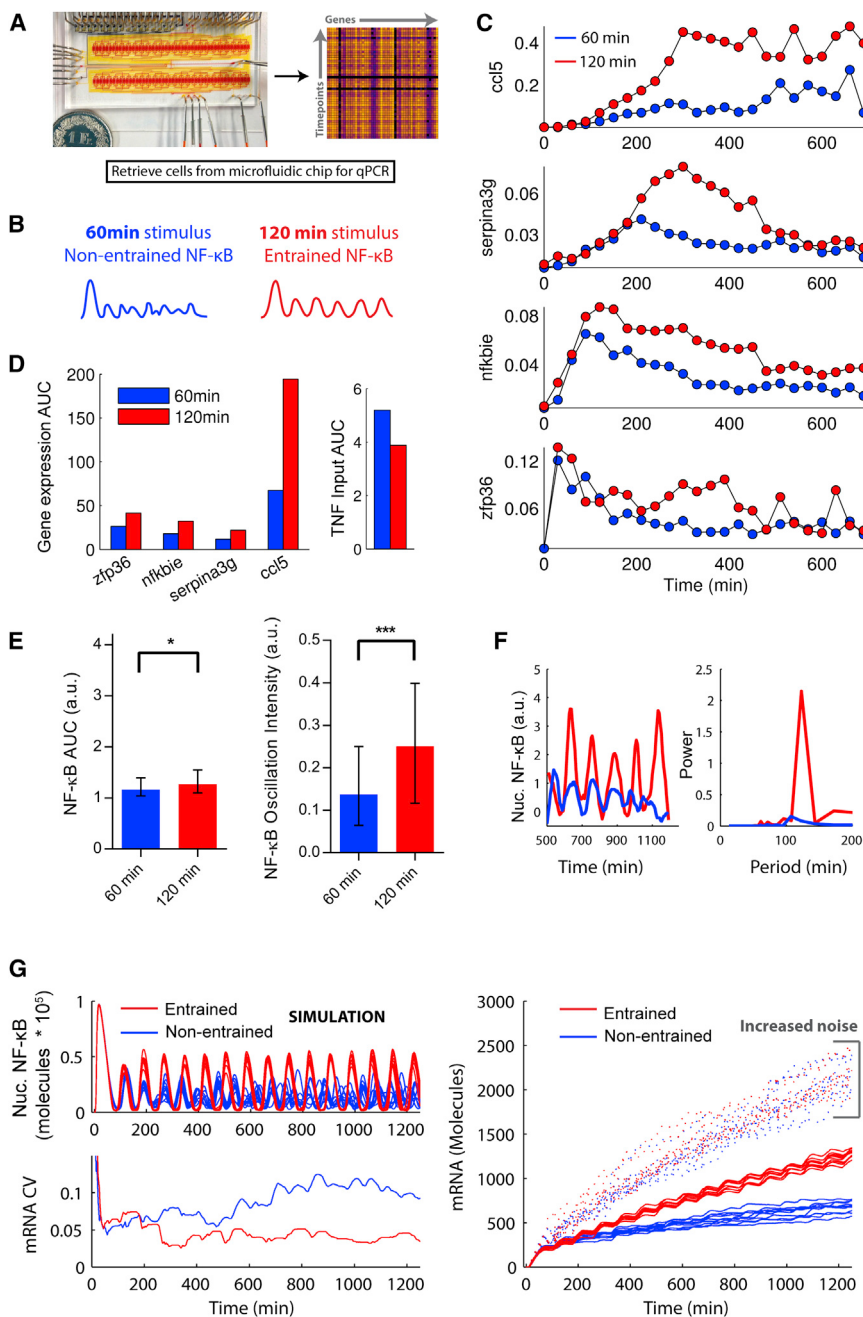


**Figure 3. Entrained NF-κB Oscillations Improve Transcriptional Efficiency**

(A) Cells are cultured and provided periodic stimulation on chip and harvested for qPCR analysis. (B) TNF stimulation with 60 min period (blue) leads to non-entrained NF-κB response, and most individual cells do not synchronize with the input. (C) NF-κB regulated gene expression under non-entrained (60 min stimulation) and entrained (120 min stimulation) conditions. Higher transcriptional output is seen when NF-κB oscillations are entrained. Enhanced transcription occurs consistently for early, middle, and late genes. The effect is most pronounced for late responding genes (i.e., *ccl5*).

(D) Gene expression output measured by area under curve (AUC). AUC is higher for entrained compared to non-entrained NF-κB response. Although 120 min stimulation increases transcript production, it is not due to higher TNF exposure, which is lower compared to 60 min stimulation. (E) Analysis of single-cell NF-κB trajectories shows modest increase in response area ( $p = 0.04$ ) and strong increase in oscillation energy ( $p = 0.0002$ ) (bars indicate median  $\pm$  interquartile range,  $p$  values by Mann-Whitney test.)

(F) Example NF-κB trajectories (for later part of time course starting at 500 min) and corresponding power spectra for 60 and 120 min input (blue and red lines, respectively), showing stronger oscillation under entrained (120 min) input. (G) Stochastic NF-κB simulation of cells under either entraining or non-entraining input (left) and gene expression output (right). Due to non-linear binding of NF-κB to DNA, stronger oscillation under entraining input creates increased gene expression output, in agreement with experiments. Increasing intrinsic noise amplifies oscillations and leads to even higher transcription output. mRNA cell-to-cell variability (measured by Coefficient of Variation, CV) is lower for entrained cells, indicating that entrainment reduces cell-to-cell mRNA variability compared to non-entrained cells.

See also Figure S2 and S3.

cell-to-cell transcription variability is significantly reduced under entraining input (Figure 3G). This result is consistent across simulated early, middle, and late-response genes (Figure S3). With reduced mRNA variability between individual cells, oscillations appear even in the population averaged experimental time course, especially in late genes (Figure 3C). Therefore, through entrainment that reduces gene regulatory and gene expression variability between cells, one may increase response homogeneity of a cell population.

These results reveal the important role for NF-κB oscillations in generating efficient transcription and indicate that periodic

signaling inputs can amplify transcriptional outputs by resonantly stimulating oscillatory pathways like NF-κB, with a beneficial role for intrinsic noise in further improving the transcriptional output.

Moreover, simulations and experiments

show reduced cell-cell variability in mRNA level for entraining input. Therefore entrainment provides a way to increase both expression output and homogeneity of a cell population.

### Stochastic Modeling Shows Noise-Enhanced NF-κB Oscillation and Entrainment

We next turned to simulations to evaluate the robustness of NF-κB entrainment to changes in the TNF input period and the influence of noise. Using the deterministic implementation of our model, we simulated periodic TNF stimulation of NF-κB in single cells and calculated entrainment ranges. In the space spanned

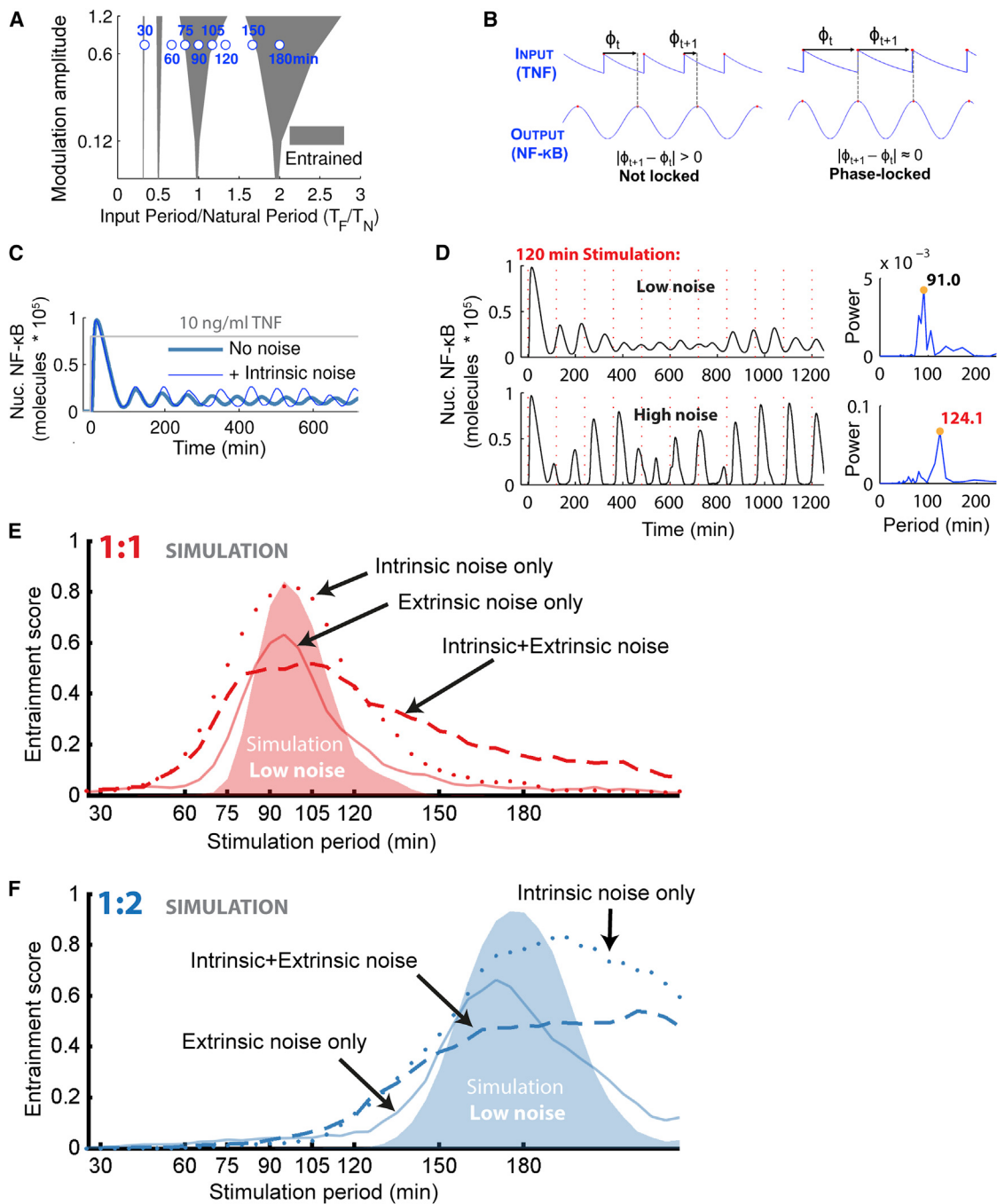


**Figure 4. Stochastic Modeling Predicts Entrainment to be Robust and that Noise Underlies Enhancement in Oscillation and Entrainment Range**

(A) Deterministic Arnold tongues (gray shaded regions) computed for decay-type TNF input show that entrainment is readily achieved in narrow regions around 90 min and 180 min ( $T_F/T_N = 1/2$ ) periodic stimulation (10 ng/ml TNF). Entrainment is also possible for 30 and 45 min input ( $T_F/T_N = 1/3, 1/2$ ). Locations of experimentally tested values are indicated by blue circles.

(B) Input-output phase relationship and phase-locking. Phase between TNF input and NF-κB output is calculated as the distance from each NF-κB peak to the start of the previous TNF cycle, normalized by the input period. When phase change between cycles is less than a threshold ( $|\phi_{t+1} - \phi_t| < 0.15$ ), input and output are considered phase-locked. Locking can occur at 1:1 ratio (one input cycle for one output cycle), or other ratios such as 1:2 (one input cycle for two output cycles).

(C) Adding intrinsic noise amplifies and sustains NF-κB oscillations in the model under constant TNF input (example single cell traces are shown).

(D) Comparison of entrainment in simulated NF-κB trajectories under low and high intrinsic noise. Under 120 min periodic TNF stimulation, high noise leads to an entrained response indicated by 120 min peak in the power spectrum. In contrast, the response under low noise is not entrained as seen in the power spectrum that shows weaker oscillations and only at the natural period.

(legend continued on next page)

by input modulation amplitude and period ( $T_F$ ), entrainment occurs in triangular regions called Arnold Tongues (Figure 4A) (Erzberger et al., 2013; Jensen and Krishna, 2012). On the edges of Arnold Tongues synchrony between the input and oscillator breaks down leading to quasiperiodic or aperiodic rhythms. Deterministic Arnold tongues for NF- $\kappa$ B indicated entrainment principally when stimulation period is near 1:1 or 1:2 ratio with the natural period and ( $T_F/T_N = 1, 2$ ) (Figure 4A), meaning that entrainment is expected when the stimulation occurs with a period near 90 min or near 180 min under 10 ng/ml TNF input.

To understand the role of different noise levels in entrainment, we simulated periodic TNF signals with varied intrinsic and extrinsic noise conditions and quantified NF- $\kappa$ B phase locking by comparing phase of the next cycle  $\phi_{t+1}$  to that of the current cycle  $\phi_t$ . If the phase difference  $|\phi_{t+1} - \phi_t|$  is less than a threshold (0.15) then the response was considered locked over that cycle (Figure 4B). Our hybrid model based on Gillespie algorithm incorporates experimentally verified intrinsic noise in TNF receptor-ligand binding, which is dominant at small TNF doses, and in transcription of  $I\kappa B\alpha$  and A20 that constitute the main negative-feedback loops leading to oscillations (Tay et al., 2010). Particularly, transcriptional noise arises from stochastic interaction of NF- $\kappa$ B transcription factors with the two copies of  $I\kappa B\alpha$  and A20 genes. We reduced the transcriptional noise by increasing the gene copy number and proportionally reducing gene expression rate per copy to maintain unchanged gene expression and similar NF- $\kappa$ B natural oscillation period between models. With the stochastic model with greatly reduced intrinsic noise, entrainment occurs for narrow regions around 90 and 180 min stimulation under high dose (10 ng/ml) TNF periodic input (Figures 4E and 4F), similar to those in the deterministic simulations. Simulations with high intrinsic noise under the same TNF input led to a significant broadening of the entrainment regions (Figures 4E and 4F, dotted line). The intrinsic noise level in these simulations was matched to the experimental level in Figure 1. High intrinsic noise in our simulations increased NF- $\kappa$ B oscillation amplitude of single cells and supported sustained oscillations needed for entrainment (Figure 4C). The power spectrum provides information about entrainment, and degree of entrainment is indicated by the relative amount of spectral power at the input period. Example simulated NF- $\kappa$ B single-cell trajectories for 120 min input are seen in Figure 4D, showing significantly increased oscillation and spectral power at the input period for the high noise case. To determine how noise effects depend on TNF dose and modulation level, we simulated the same model using computationally efficient stochastic differential equations, which showed that intrinsic noise improves NF- $\kappa$ B power at input period when the input modulation is smaller (i.e., weaker driving stimuli), as in higher-dose periodic TNF stimulation (Figure S4).

Extrinsic noise generates cell-to-cell variability in NF- $\kappa$ B natural period (Figures 1G and 1H). When the natural period in an individual cell is sufficiently close to the TNF input period,

entrainment will occur. Extrinsic noise in the system thus increases the probability that at least a portion of cells in the population will entrain to a given input. When we included extrinsic in addition to intrinsic noise in our simulations, we observed a further broadening of entrainment ranges NF- $\kappa$ B (Figures 4E and 4F). Overall, these simulations indicate that extrinsic and intrinsic noise together enable cells to entrain and drive efficient transcriptional responses for a wider range of dynamical inputs.

### NF- $\kappa$ B Entrainment Range Is Very Broad as Predicted by Noisy Simulations

To experimentally test the robustness of NF- $\kappa$ B entrainment to changes in the input, we applied TNF inputs with 30 to 180 min periods to fibroblasts cultured in separate chambers of the microfluidic system, under three different TNF doses of 10, 0.5, and 0.1 ng/ml (Figures 5 and S5). The dataset contains analysis of approximately 2,000 cells over 24 hrs duration measured every 5 min, creating more than half a million data points (Movies S2, S3, and S4). Heatmaps with one row for each single-cell NF- $\kappa$ B trajectory show population synchrony that improves with time (Figure 5A). Periodic stimulation with reduced dose leads to even better entrainment (Figure 5A). The fraction of NF- $\kappa$ B cycles locking to different entrainment ratios was computed for each stimulation condition, and as anticipated 1:1 locking is maximized when the stimulation period is near 90 min and 1:2 locking is maximized for 180 min stimulation (Figure 5B). Surprisingly, we observed cells having entrained oscillations in every input period tested, even in those inputs like 120 min that are not predicted by the deterministic or low noise simulations. Good agreement is seen between experimental entrainment values and high-noise model simulations (both under 10 ng/ml TNF dose) incorporating both extrinsic and intrinsic noise (Figure 5B). We did not observe dependence on cell density (Figure S6).

A consequence of natural period diversity is entrainment heterogeneity, including the ability for different cells in the population to entrain at different ratios. Cells entrained at multiple ratios or did not entrain and exhibited quasiperiodic oscillation (Figure 6C). Period probability follows a multimodal distribution, indicating simultaneous mixture of for example 1:1 and 1:2 locking responses in the population (Figure 6A). Simulations incorporating only extrinsic noise also generate mixed locking responses, indicating that locking heterogeneity can arise from extrinsic noise (Figure 6D).

Period distributions show narrowing with reduced TNF dose, supporting more effective entrainment (Figure 6B). Comparing mean pairwise Spearman correlation for population responses at each input revealed increased correlation as dose decreases and at larger input periods (Figure 6E). Therefore, NF- $\kappa$ B is more amenable to entrainment for input level in middle of its dose dynamic range (Tay et al., 2010) in agreement with simulation (Figure S5C). Entrainment is more efficient under input periods larger than 60 min, and frequencies larger than  $0.02 \text{ min}^{-1}$  (50 min

(E and F) Entrainment simulation: Under low-noise simulation (extrinsic noise off, intrinsic noise reduced), entrainment occurs for narrow regions around 90 min stimulation period (1:1 entrainment, E) and around 180 min period (1:2 entrainment, F). Increasing intrinsic noise in the model broadens regions of entrainment (dotted line). Extrinsic noise alone also increases entrainment range for the population. Adding both extrinsic and intrinsic noise further expands entrainment. See also Figure S4.

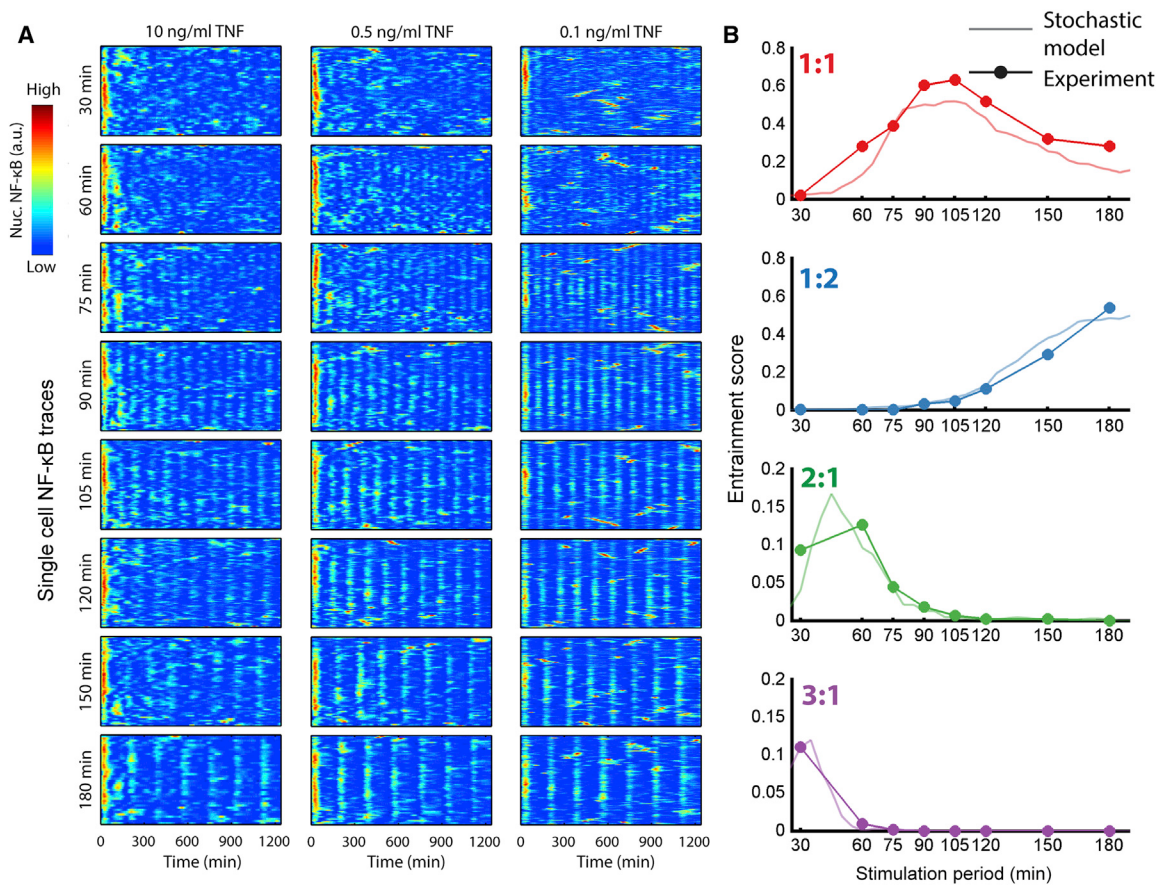


**Figure 5. NF-κB Entrainment Range Is Wide and Agrees with Noisy Model Predictions**

(A) Heatmaps of single-cell NF-κB trajectories under different doses of TNF (10, 0.5, and 0.1 ng/ml) for stimulation periods ranging from 30 to 180 min. Color indicates NF-κB intensity from low (blue) to high (red). Entrainment of individual cells can be visualized with the appearance of well-aligned peaks. Entrainment and synchronization is pronounced for 90 and 180 min stimulation. Reduced dose leads to greater oscillation synchrony and improved entrainment across all stimulation periods (Figure S5B).

(B) Comparison of entrainment scores for 10 ng/ml stimulation in various locking modes shows agreement between experiments and noisy model prediction. See also Figure S5.

period) are not observed in the single cell power spectra, indicating that NF-κB system acts like a filter that prevents transmission of rapid TNF input fluctuations into transcription.

## DISCUSSION

Here, we provide insight into the function of transcription factor dynamics and noise in gene expression control under fluctuating signaling inputs. Sustained, heterogeneous single-cell NF-κB oscillations synchronize to an oscillating TNF signal in a wide range of stimulation frequencies and become entrained. Entrainment causes amplification of NF-κB oscillations and increased gene expression (Figure 7). Simulations predict that both intrinsic and extrinsic noise can improve NF-κB entrainment range, allowing cells to respond synchronously to broader range of inflammatory signals (Figure 4). Single-cell measurements confirmed that indeed NF-κB entrainment occurs in the broad range as predicted by stochastic modeling (Figure 5). While extrinsic noise leads to differences in oscillation frequency between cells

creating heterogeneous locking behavior and increases entrainment robustness of the population to changes in input period, a surprising finding is the beneficial role for intrinsic noise in dynamical signaling: molecular fluctuation arising from low copy-number feedback transcripts (IkB and A20) can act to enhance NF-κB oscillation and expand the range of inputs that entrain NF-κB and ultimately enhance target gene expression (Figure 7). Increased gene expression was explained by incorporating data on non-linear NF-κB-DNA binding affinity into the model, and we see the greatest differential regulation for late genes such as Ccl5 in agreement with findings that late genes are more sensitive to oscillatory regulation (Ashall et al., 2009; Wee et al., 2012).

Together, our results describe important functions for oscillation and noise in signaling networks. Transcription factor oscillation allows amplified pathway output in response to a periodic stimulus and thus increases system efficiency by reducing the amount of input signal needed to generate strong response. Oscillation moreover allows control of heterogeneity through

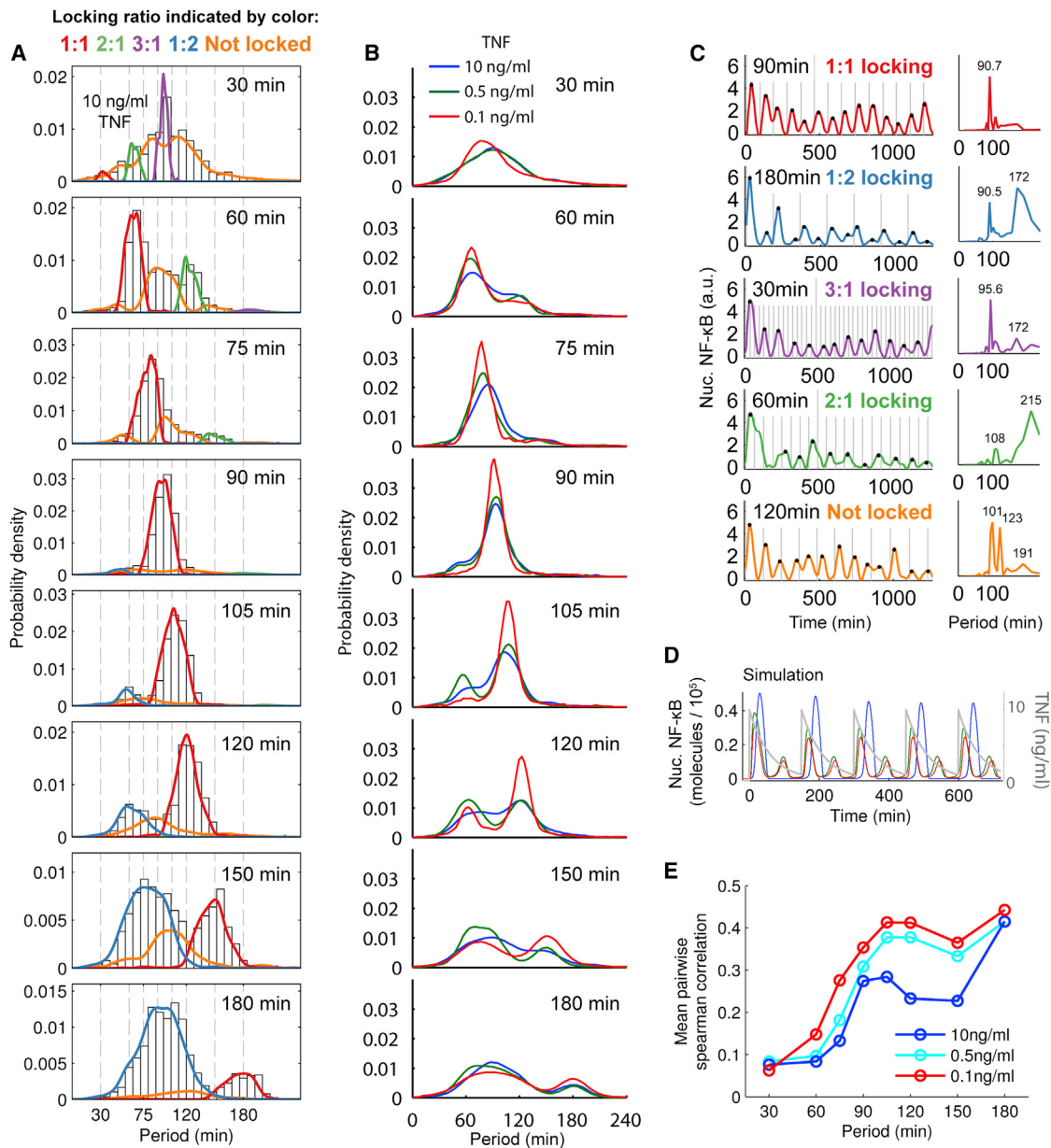


**Figure 6. Population Heterogeneity and Dose Dependence of NF-κB Entrainment**

- (A) Period probability distributions for 10 ng/ml TNF input reveal entrainment at multiple ratios between the input and output period. Under 90 min input, the population entrains nearly homogeneously with a 90 min phase-locked oscillation (1:1 ratio, red line). In contrast, during 150 min stimulation cells may respond with a 150 min oscillation (1:1 ratio, red line), or a 75 min oscillation (1:2 ratio, blue line), or without phase-locking (orange line).
- (B) Period distributions for multiple TNF concentrations. Lower concentration leads to period distribution narrowing, indicating improved entrainment and reduced cell-to-cell variability.
- (C) Measured single-cell NF-κB traces and power spectra for each locking ratio and an example quasiperiodic response (Not locked).
- (D) Simulation with extrinsic noise shows that different locking ratios may occur simultaneously (blue line – 1:1 locking, red and green lines – 1:2 locking).
- (E) Mean pairwise spearman correlation in NF-κB dynamics indicating better population entrainment at lower input concentration and at higher input periods. The NF-κB system efficiently filters rapid input fluctuations with periods shorter than 50 min.

See also Figure S6.

synchronization of gene regulatory dynamics across the population. By enhancing oscillation and entrainment bandwidth, noise facilitates efficient transcription in dynamic signaling contexts.

Cytokines like TNF activate multiple signaling pathways, and resonant pathway stimulation provides a way to achieve specific responses. A low-dose signal, delivered periodically, could excite NF-κB oscillations and activate NF-κB signaling while

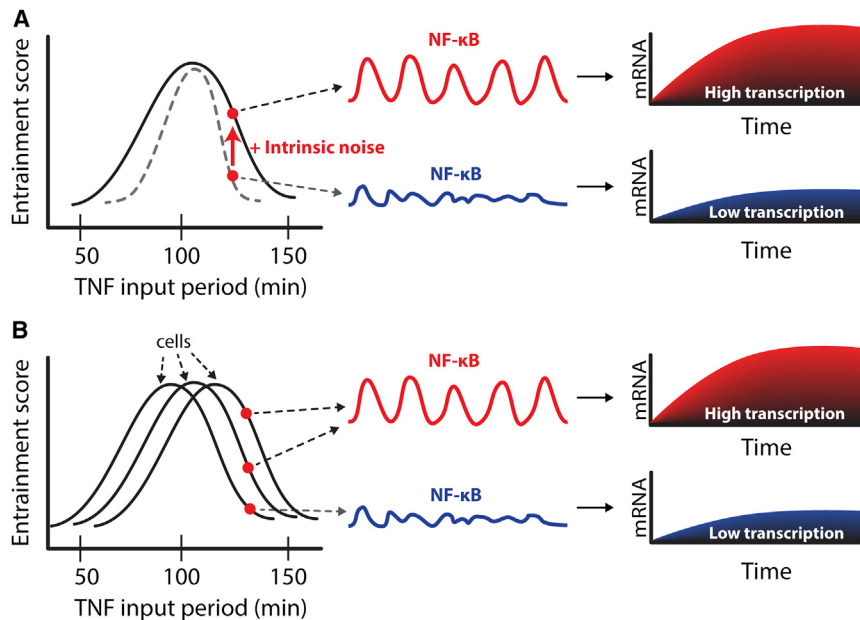


**Figure 7. Role of Intrinsic and Extrinsic Noise in NF-κB Entrainment and Enhanced Gene Expression**

(A and B) Entrainment score for different inputs shown on the left side; single-cell NF-κB time course shown in the middle; and the corresponding mRNA output is shown on the right. (A) Black curve on the left shows the entrainment range of a given cell with intrinsic noise, and dashed gray curve shows the narrower noise-free entrainment range. Signaling inputs at the edge of the entrainment range cause non-entrained NF-κB responses and small amplitude (in blue), resulting in impaired gene expression output. Intrinsic noise improves the amplitude and the regularity of NF-κB oscillations (in red), resulting in increased gene expression output. Intrinsic noise can increase entrainment score and also the bandwidth, where cells entrain to a broader range of input periods. (B) Extrinsic noise creates cell-to-cell variability in the entrainment range, resulting in a broader entrainment bandwidth for the population. Population variability in entrainment potential ensures that at least some cells will entrain under a given input period.

avoiding activation of non-oscillatory pathways (such as AP-1). Entrainment with resonance also allows more efficient communication. Indeed, we show that a periodic resonant stimulus achieves greater pathway output while at the same time requiring fewer TNF molecules than a non-entraining stimulus.

Oscillation with resonance may act as a filter. Non-entraining inputs like rapid TNF fluctuations are effectively attenuated at the gene expression level. This may allow NF-κB system to filter out fast cytokine fluctuations that are not physiological (i.e., input noise). While NF-κB exhibits a robust natural period of ~90 min, researchers are finding oscillation in many signaling pathways with differing characteristic frequencies. Therefore the pathway specificity of a pleiotropic factor such as TNF might be tuned by changing the frequency with which it stimulates a cell. Nonetheless, it is likely that oscillatory pathways are linked within and between cells more than is currently appreciated (Kupzig et al., 2005), and temporal filtering allows cells to achieve specific responses based on the frequency content of input signals.

NF-κB both responds to and drives cytokine production, and oscillatory cytokine production has been observed in activated single T cells (Han et al., 2012). Entrainment of NF-κB could be a coordination mechanism during infection, by controlling paracrine signals that instruct migration or fate determination of immune cells (Yde et al., 2011). TNF-positive feedback in secretory immune cells such as macrophages could improve entrainment at higher cell density, creating a more amplified (and more homogeneous) response (Pekalski et al., 2013). The broad entrainment range of the NF-κB system allows cells to adapt their oscillation frequency and gene expression dynamics to match cytokine fluctuation in the environment.

Our findings suggest a surprising role for noise and oscillation in mammalian signal transduction and transcriptional control (Figure 7). In dynamic, physiological signaling scenarios oscillation provides cells the ability to decode not only the amplitude

but also frequency content of input signals. Inputs occurring near the natural frequency of an oscillatory system are amplified and generate higher gene expression output, while other input frequencies generate an attenuated response. By enhancing oscillation and entrainment at small signal modulation noise may improve the transfer of weaker dynamic signals in the NF-κB system. Entrainment allows efficient cell-cell communication, control of cell-cell heterogeneity, and possibility to selectively activate oscillatory pathways through resonant stimulation. The prevalence of oscillation in signaling networks suggests that cells are well-equipped for processing dynamic signals.

## EXPERIMENTAL PROCEDURES

### TNF- $\alpha$ Stimulation Using Microfluidic Cell Culture

We use the cell culture chip described previously (Gómez-Sjöberg et al., 2007). Cells were seeded in PDMS chambers coated with fibronectin at constant density ~20,000 cells/cm<sup>2</sup> and were cultured overnight prior to stimulation. Standard culture conditions of 5% CO<sub>2</sub> and 37°C were maintained using an incubation chamber. Mouse TNF- $\alpha$  (Invitrogen) was diluted in DMEM media in vials pressured with 5% CO<sub>2</sub> and kept on ice. Microbore tubing (PEEK, Idex) connected the TNF- $\alpha$  supply to the chip. For continuous pumping input, the on-chip peristaltic pump was operated at a flow rate ~200 nl/min. For periodic input, TNF- $\alpha$  containing media was introduced and incubated in the chamber, allowing degradation and internalization of the ligand. The chamber volume is replaced with fresh TNF- $\alpha$  containing media at defined intervals, leading to periodic sawtooth pattern in ligand concentration.

### Cell Retrieval and Gene Expression Analysis

Cells were loaded into the cell culture chip, and a Matlab program delivered 60 min or 120 min periodic inputs with start times staggered by 30 min to generate time points from 0 to 23.5 hr. Cells in one chamber (approximately 200 cells) were retrieved for each time point. At the conclusion of stimulation, cells in all chambers were lysed at once on-chip, and retrieved in a 2  $\mu$ l volume of lysis buffer using an automated routine. Cells exited the chip through ~10 cm length microbore tubing positioned into wells of a 96-well plate. Wash steps using PBS prior to retrieval prevented cross-contamination of

chambers. cDNA was synthesized using Cells Direct One Step RT-PCR kit (In-vitrogen). TaqMan primers and probes (Applied Biosystems) were used for real-time qPCR. Gene expression was assayed using the 48.48 Dynamic Array IFC chip (Fluidigm). Cycle thresholds (CT) were converted to relative expression values normalized to GAPDH ( $2^{(Ct_{gapdh} - Ct_{gene})}$ ). Total expression abundance was calculated as the integral of the relative expression (using the Matlab *trapz* function).

### Image Acquisition and Data Processing

The microfluidic chip was mounted on an automated Leica DMI6000B microscope, and fluorescence images (red and green channels for p65 and H2B reporters, respectively) were acquired at 20 $\times$  magnification via a Retiga-SRV CCD camera (QImaging) every 5–6 min for 24–48 hr. CellProfiler software ([www.cellprofiler.org](http://www.cellprofiler.org)) and custom Matlab routines (Gómez-Sjöberg et al., 2007) were used for image processing (available on request). NF- $\kappa$ B activation was quantified as mean nuclear fluorescence intensity after background correction. Area-under-curve provides a measure of total NF- $\kappa$ B activity (Tay et al., 2010) and was quantified as the integral of the NF- $\kappa$ B response (using Matlab *trapz*). For peak analysis and heatmaps data were smoothed and standardized (Matlab functions *smooth* and *zscore*) followed by peak detection (Matlab *mspeaks*). Peak-to-peak distances were computed as the difference between peak times (Matlab *diff*). Cell image overlays aided visualization of oscillation peaks (colored green) and troughs (colored red).

### NF- $\kappa$ B Reporter Cell Line

Mouse (3T3) fibroblasts expressing near-endogenous p65 levels were described previously (Tay et al., 2010). Briefly, p65 $^{-/-}$  mouse 3T3 fibroblasts were engineered to express p65-DsRed under control of 1.5 kb p65 promoter sequence (Lee et al., 2009; Tay et al., 2010). A clone was selected with minimum detectable fluorescence intensity to achieve near-endogenous expression level and NF- $\kappa$ B dynamics similar to wild-type (Lee et al., 2009). Addition of ubiquitin-promoter driven H2B-GFP expression provided a nuclear label to facilitate automated tracking and image processing.

### SUPPLEMENTAL INFORMATION

Supplemental Information includes Extended Experimental Procedures, six figures, and four movies and can be found with this article online at <http://dx.doi.org/10.1016/j.cell.2015.01.013>.

### ACKNOWLEDGMENTS

We acknowledge Tomasz Lipniacki, Mustafa Khammash, Benjamin Hepp, and Ankit Gupta for discussions on NF- $\kappa$ B and transcription modeling, and Kobi Benenson and Alexander Hoffmann for commenting on the manuscript. S.T. acknowledges European Union ERC Starting Grant (SingleCellDynamics), Swiss Nationalfonds, SNF SystemsX, and NCCR Molecular Systems Engineering for funding support.

Received: August 18, 2014

Revised: November 2, 2014

Accepted: January 5, 2015

Published: January 29, 2015

### REFERENCES

- Abraham, U., Granada, A.E., Westerman, P.O., Heine, M., Kramer, A., and Herzel, H. (2010). Coupling governs entrainment range of circadian clocks. *Mol. Syst. Biol.* 6, 438.
- Albeck, J.G., Mills, G.B., and Brugge, J.S. (2013). Frequency-modulated pulses of ERK activity transmit quantitative proliferation signals. *Mol. Cell* 49, 249–261.
- Ashall, L., Horton, C.A., Nelson, D.E., Paszek, P., Harper, C.V., Sillitoe, K., Ryan, S., Spiller, D.G., Unitt, J.F., Broomhead, D.S., et al. (2009). Pulsatile stimulation determines timing and specificity of NF- $\kappa$ pA/B-dependent transcription. *Science* 324, 242–246.
- Berridge, M.J., Bootman, M.D., and Roderick, H.L. (2003). Calcium signalling: dynamics, homeostasis and remodelling. *Nat. Rev. Mol. Cell Biol.* 4, 517–529.
- Cai, L., Dalal, C.K., and Elowitz, M.B. (2008). Frequency-modulated nuclear localization bursts coordinate gene regulation. *Nature* 455, 485–490.
- Cheong, R., Rhee, A., Wang, C.J., Nemenman, I., and Levchenko, A. (2011). Information transduction capacity of noisy biochemical signaling networks. *Science* 334, 354–358.
- Collins, J.J., Imhoff, T.T., and Grigg, P. (1996). Noise-enhanced information transmission in rat SA1 cutaneous mechanoreceptors via aperiodic stochastic resonance. *J. Neurophysiol.* 76, 642–645.
- Dolmetsch, R.E., Xu, K., and Lewis, R.S. (1998). Calcium oscillations increase the efficiency and specificity of gene expression. *Nature* 392, 933–936.
- Douglass, J.K., Wilkens, L., Pantazelou, E., and Moss, F. (1993). Noise enhancement of information transfer in crayfish mechanoreceptors by stochastic resonance. *Nature* 365, 337–340.
- Eldar, A., and Elowitz, M.B. (2010). Functional roles for noise in genetic circuits. *Nature* 467, 167–173.
- Elowitz, M.B., Levine, A.J., Siggia, E.D., and Swain, P.S. (2002). Stochastic gene expression in a single cell. *Science* 297, 1183–1186.
- Erzberger, A., Hampp, G., Granada, A.E., Albrecht, U., and Herzel, H. (2013). Genetic redundancy strengthens the circadian clock leading to a narrow entrainment range. *J. R. Soc. Interface* 10, 20130221.
- Falcke, M. (2003). Deterministic and stochastic models of intracellular Ca<sup>2+</sup>-waves. *New J. Physics* 5, 96.
- Gérard, C., and Goldbeter, A. (2012). Entrainment of the mammalian cell cycle by the circadian clock: modeling two coupled cellular rhythms. *PLoS Comput. Biol.* 8, e1002516.
- Goldbeter, A., and Pourquié, O. (2008). Modeling the segmentation clock as a network of coupled oscillations in the Notch, Wnt and FGF signaling pathways. *J. Theor. Biol.* 252, 574–585.
- Goldbeter, A., Li, Y., and Dupont, G. (1990). Oscillatory dynamics in intercellular communication. *Biomed. Biochim. Acta* 49, 935–940.
- Gómez-Sjöberg, R., Leyrat, A.A., Pirone, D.M., Chen, C.S., and Quake, S.R. (2007). Versatile, fully automated, microfluidic cell culture system. *Anal. Chem.* 79, 8557–8563.
- Han, Q., Bagheri, N., Bradshaw, E.M., Hafler, D.A., Lauffenburger, D.A., and Love, J.C. (2012). Polyfunctional responses by human T cells result from sequential release of cytokines. *Proc. Natl. Acad. Sci. USA* 109, 1607–1612.
- Hao, S., and Baltimore, D. (2013). RNA splicing regulates the temporal order of TNF-induced gene expression. *Proc. Natl. Acad. Sci. USA* 110, 11934–11939.
- Hayden, M.S., and Ghosh, S. (2008). Shared principles in NF- $\kappa$ pA/B signaling. *Cell* 132, 344–362.
- Hoffmann, A., Levchenko, A., Scott, M.L., and Baltimore, D. (2002). The IkappaB-NF- $\kappa$ pA/B Signaling Module: Temporal Control and Selective Gene Activation (New York, NY: Science), pp. 1–5.
- Huh, D., and Paulsson, J. (2011). Random partitioning of molecules at cell division. *Proc. Natl. Acad. Sci. USA* 108, 15004–15009.
- Jensen, M.H., and Krishna, S. (2012). Inducing phase-locking and chaos in cellular oscillators by modulating the driving stimuli. *FEBS Lett.* 586, 1664–1668.
- Junkin, M., and Tay, S. (2014). Microfluidic single-cell analysis for systems immunology. *Lab Chip* 14, 1246–1260.
- Kageyama, R., Ohtsuka, T., Shimojo, H., and Imayoshi, I. (2008). Dynamic Notch signaling in neural progenitor cells and a revised view of lateral inhibition. *Nat. Neurosci.* 11, 1247–1251.
- Kellogg, R.A., Gómez-Sjöberg, R., Leyrat, A.A., and Tay, S. (2014). High-throughput microfluidic single-cell analysis pipeline for studies of signaling dynamics. *Nat. Protoc.* 9, 1713–1726.
- Kupzig, S., Walker, S.A., and Cullen, P.J. (2005). The frequencies of calcium oscillations are optimized for efficient calcium-mediated activation of Ras and the ERK/MAPK cascade. *Proc. Natl. Acad. Sci. USA* 102, 7577–7582.

- Lee, T.K., Denny, E.M., Sanghvi, J.C., Gaston, J.E., Maynard, N.D., Hughey, J.J., and Covert, M.W. (2009). A noisy paracrine signal determines the cellular NF- $\kappa$ B response to lipopolysaccharide. *Sci. Signal.* 2, ra65.
- Leloup, J.C., and Goldbeter, A. (2003). Toward a detailed computational model for the mammalian circadian clock. *Proc. Natl. Acad. Sci. USA* 100, 7051–7056.
- Levine, J.H., Lin, Y., and Elowitz, M.B. (2013). Functional roles of pulsing in genetic circuits. *Science* 342, 1193–1200.
- Lindner, B., Garcia-Ojalvo, J., Neiman, A., and Schimansky-Geier, L. (2004). Effects of noise in excitable systems. *Phys. Rep.* 392, 321–424.
- Lipniacki, T., Paszek, P., Brasier, A.R., Luxon, B., and Kimmel, M. (2004). Mathematical model of NF- $\kappa$ B regulatory module. *J. Theor. Biol.* 228, 195–215.
- Lipniacki, T., Puszynski, K., Paszek, P., Brasier, A.R., and Kimmel, M. (2007). Single TNF $\alpha$  trimers mediating NF- $\kappa$ B activation: stochastic robustness of NF- $\kappa$ B signaling. *BMC Bioinformatics* 8, 376.
- Little, J.W., Shepley, D.P., and Wert, D.W. (1999). Robustness of a gene regulatory circuit. *EMBO J.* 18, 4299–4307.
- Longo, D.M., Selimkhanov, J., Kearns, J.D., Hasty, J., Hoffmann, A., and Tsimring, L.S. (2013). Dual delayed feedback provides sensitivity and robustness to the NF- $\kappa$ B signaling module. *PLoS Comput. Biol.* 9, e1003112.
- McDonnell, M.D., and Ward, L.M. (2011). The benefits of noise in neural systems: bridging theory and experiment. *Nat. Rev. Neurosci.* 12, 415–426.
- Mondragón-Palomino, O., Danino, T., Selimkhanov, J., Tsimring, L., and Hasty, J. (2011). Entrainment of a population of synthetic genetic oscillators. *Science* 333, 1315–1319.
- Mori, T., and Kai, S. (2002). Noise-induced entrainment and stochastic resonance in human brain waves. *Phys. Rev. Lett.* 88, 218101.
- Nelson, D.E., Ihekweazu, A.E.C., Elliott, M., Johnson, J.R., Gibney, C.A., Foreman, B.E., Nelson, G., See, V., Horton, C.A., Spiller, D.G., et al. (2004). Oscillations in NF- $\kappa$ B signaling control the dynamics of gene expression. *Science* 306, 704–708.
- Paszek, P., Ryan, S., Ashall, L., Sillitoe, K., Harper, C.V., Spiller, D.G., Rand, D.A., and White, M.R. (2010). Population robustness arising from cellular heterogeneity. *Proc. Natl. Acad. Sci. USA* 107, 11644–11649.
- Pękalski, J., Zuk, P.J., Kochanczyk, M., Junkin, M., Kellogg, R., Tay, S., and Lipniacki, T. (2013). Spontaneous NF- $\kappa$ B activation by autocrine TNF $\alpha$  signaling: a computational analysis. *PLoS ONE* 8, e78887.
- Perc, M., and Marhl, M. (2003). Noise enhances robustness of intracellular Ca $^{2+}$  oscillations. *Phys. Lett. A* 316, 304–310.
- Phelps, C.B., Sengchanthalangsy, L.L., Malek, S., and Ghosh, G. (2000). Mechanism of kappa B DNA binding by Rel/NF- $\kappa$ B dimers. *J. Biol. Chem.* 275, 24392–24399.
- Pikovsky, A., Rosenblum, M., and Kurths, J. (2003). Synchronization: a universal concept in nonlinear sciences, Volume 12 (Cambridge: Cambridge University Press).
- Purvis, J.E., and Lahav, G. (2013). Encoding and decoding cellular information through signaling dynamics. *Cell* 152, 945–956.
- Purvis, J.E., Karhohs, K.W., Mock, C., Batchelor, E., Loewer, A., and Lahav, G. (2012). p53 dynamics control cell fate. *Science* 336, 1440–1444.
- Reppert, S.M., and Weaver, D.R. (2002). Coordination of circadian timing in mammals. *Nature* 418, 935–941.
- Schütze, J., Mair, T., Hauser, M.J.B., Falcke, M., and Wolf, J. (2011). Metabolic synchronization by traveling waves in yeast cell layers. *Biophys. J.* 100, 809–813.
- Shankaran, H., Ippolito, D.L., Chrisler, W.B., Resat, H., Bollinger, N., Opresko, L.K., and Wiley, H.S. (2009). Rapid and sustained nuclear-cytoplasmic ERK oscillations induced by epidermal growth factor. *Mol. Syst. Biol.* 5, 332.
- Süel, G.M., Garcia-Ojalvo, J., Liberman, L.M., and Elowitz, M.B. (2006). An excitable gene regulatory circuit induces transient cellular differentiation. *Nature* 440, 545–550.
- Swain, P.S., Elowitz, M.B., and Siggia, E.D. (2002). Intrinsic and extrinsic contributions to stochasticity in gene expression. *Proc. Natl. Acad. Sci. USA* 99, 12795–12800.
- Tay, S., Hughey, J.J., Lee, T.K., Lipniacki, T., Quake, S.R., and Covert, M.W. (2010). Single-cell NF- $\kappa$ B dynamics reveal digital activation and analogue information processing. *Nature* 466, 267–271.
- Turner, D.A., Paszek, P., Woodcock, D.J., Nelson, D.E., Horton, C.A., Wang, Y., Spiller, D.G., Rand, D.A., White, M.R., and Harper, C.V. (2010). Physiological levels of TNF $\alpha$  stimulation induce stochastic dynamics of NF- $\kappa$ B responses in single living cells. *J. Cell Sci.* 123, 2834–2843.
- Varela, F., Lachaux, J.P., Rodriguez, E., and Martinerie, J. (2001). The brain-web: phase synchronization and large-scale integration. *Nat. Rev. Neurosci.* 2, 229–239.
- Vilar, J.M., Kueh, H.Y., Barkai, N., and Leibler, S. (2002). Mechanisms of noise-resistance in genetic oscillators. *Proc. Natl. Acad. Sci. USA* 99, 5988–5992.
- Wakamoto, Y., Dhar, N., Chait, R., Schneider, K., Signorino-Gelo, F., Leibler, S., and McKinney, J.D. (2013). Dynamic persistence of antibiotic-stressed mycobacteria. *Science* 339, 91–95.
- Wang, Y., Paszek, P., Horton, C.A., Kell, D.B., White, M.R., Broomhead, D.S., and Muldoon, M.R. (2011). Interactions among oscillatory pathways in NF- $\kappa$ B signaling. *BMC Syst. Biol.* 5, 23.
- Wee, K.B., Yio, W.K., Surana, U., and Chiam, K.H. (2012). Transcription factor oscillations induce differential gene expressions. *Biophys. J.* 102, 2413–2423.
- Yang, Q., Pando, B.F., Dong, G., Golden, S.S., and van Oudenaarden, A. (2010). Circadian gating of the cell cycle revealed in single cyanobacterial cells. *Science* 327, 1522–1526.
- Yde, P., Mengel, B., Jensen, M.H., Krishna, S., and Trusina, A. (2011). Modeling the NF- $\kappa$ B mediated inflammatory response predicts cytokine waves in tissue. *BMC Syst. Biol.* 5, 115.
- Yissachar, N., Sharar Fischler, T., Cohen, A.A., Reich-Zeliger, S., Russ, D., Shifrut, E., Porat, Z., and Friedman, N. (2013). Dynamic response diversity of NFAT isoforms in individual living cells. *Mol. Cell* 49, 322–330.
- Yoshiura, S., Ohtsuka, T., Takenaka, Y., Nagahara, H., Yoshikawa, K., and Kageyama, R. (2007). Ultradian oscillations of Stat, Smad, and Hes1 expression in response to serum. *Proc. Natl. Acad. Sci. USA* 104, 11292–11297.
- Zhou, C., Kurths, J., Kiss, I.Z., and Hudson, J.L. (2002). Noise-enhanced phase synchronization of chaotic oscillators. *Phys. Rev. Lett.* 89, 014101.